International Journal of Structural Stability and
Dynamics Vol. 16 (2016) 1550016 (18 pages)
World Scientific Publishing Company
DOI: 10.1142/S0219455415500169

APPLICATION OF KALMAN FILTERING METHODS TO ONLINE REAL-TIME STRUCTURAL IDENTIFICATION: A COMPARISON STUDY

MOHSEN ASKARI
Corresponding Author
Center for Built Infrastructure Research, University of Technology Sydney
P.O. Box 123, Broadway, NSW 2007, Australia
Mohsen.Askari@uts.edu.au

JIANCHUN LI
Center for Built Infrastructure Research, University of Technology Sydney, Australia
Jianchun.Li@uts.edu.au

BIJAN SAMALI
Institute for Infrastructure Engineering, University of Western Sydney, Australia
B.Samali@uws.edu.au

System identification refers to the process of building or improving mathematical models of dynamical systems from the observed experimental input–output data. In the area of civil engineering, the estimation of the integrity of a structure under dynamic loadings and during service condition has become a challenge for the engineering community. Therefore, there has been a great deal of attention paid to online and real-time structural identification, especially when input-output measurement data are contaminated by high-level noise. Among real-time identification methods, one of the most successful and widely used algorithms for estimation of system states and parameters is the Kalman filter and its various nonlinear extensions such as Extended Kalman Filter (EKF), Iterated Extended Kalman Filter (IEKF), the recently developed Unscented Kalman Filter (UKF) and Iterated Unscented Kalman Filter (IUKF). In this paper, an investigation has been carried out on the aforementioned techniques for their effectiveness and efficiencies through a highly nonlinear SDOF structure as well as a two-storey linear structure. Although IEKF is an improved version of EKF, results show that IUKF generally produces better results in terms of structural parameters and state estimation than UKF and IEKF. Also IUKF is more robust to noise levels compared to the other approaches.

Keywords: Online system identification, structural identification, extended Kalman filter, iterated extended Kalman filter, unscented Kalman filter, iterated unscented Kalman filter.

1. Introduction

Our buildings and infrastructure have been always susceptible to natural or man-made hazards. Therefore, it has prompted governments and the research community to find a realistic way for protecting civil infrastructure and community from hazards such as earthquakes, winds, aging, deterioration, and poor quality construction. Consequently, many works have been done by engineers in the past decades to find practical solutions to this problem. This has led to two main areas of research, i.e. structural control and structural health monitoring (SHM).

SHM is defined as identification of the existence, location and severity of likely damage in a structure by comparing the current state of the structure relative to the intact structure's baseline state. The traditional experimental based damage detection methods need subjective visual inspection of the structure. On the other hand, SHM does not require this and therefore, it can provide valuable information for post-event safety assessments of the structure.

Farrar and Worden[1] described SHM as a four-part process: operational evaluation, data acquisition, feature extraction, and statistical model development. Operational evaluation determines economic and/or life safety issues, damage definitions, conditions, both operational and environmental, under which the system functions, and, finally, limitations on data acquisition in the operational environment. Data acquisition includes determination and measurements of required quantities, type of sensors, location, number, resolution, and bandwidth, and also finding the right sampling time for data collection. The third part in SHM is feature extraction, which is the process of parameters identification from collected data to determine existence, location, type, and the extent of damage. Most traditional identification techniques, however, require measurements of excitation (input) and response (output) in order to produce the required data for model identification. In order to obtain such measurement data, controlled tests are needed to be conducted on the structure under investigation. For instance, in multi-input-multi-output (MIMO) modal testing, a common way to collect the required data is to excite a testing structure by applying known excitations at several points and measure the response of structure at the sensor locations [2]. However, for many civil engineering structures, it may be difficult or not feasible to provide such artificial excitations because of their sheer size, geometry and location or simply due to interruption to normal service such as in case of bridges. Moreover, providing such an external energy to excite a large civil structure to gain the proposed level of vibration may not be practical.

On the other hand, civil structures in their operational condition inevitably experience various unmeasurable dynamic loadings such as wind, earthquake and traffic. Measurements of structural responses under such loadings can be used for identification of structural parameters or structural models. If such identification is carried out after collection of the entire data sets, the identification techniques is called off-line method which is useful when the final state of the structure at the end of loading is important. The off-line algorithms have been used widely in engineering problems in the last decades. [3, 4, 5] However, in some cases, real-time system identification is absolutely necessary. For example, in structural control, during severe loadings such as earthquakes, access to the updated structural model in order to produce optimal control actions requires real-time structural identification.

Among many proposed SHM techniques in the literature, only a few, such as adaptive H_∞ filter techniques [6], bootstrap filtering approaches [7], Artificial Neural Networks (ANNs) based methods [8, 9, 10, 11], wavelet approaches [12], are suitable for real-time problems. However, they are associated with significant computational cost and complexity, or are incapable of locating and quantifying the damage detected. Therefore, developing on-line SHM techniques with simpler and more suitable algorithms is still a challenge.

Kalman filtering methods is one of the groups of parametric methods which have been widely used in engineering online identification problems. A variety of Kalman filtering techniques, including extended Kalman filter (EKF) and unscented Kalman filter (UKF) have been proposed to estimate both response and parameters of the mechanical models [13].

Hoshiya and Saito[14] utilised an extended Kalman filter for system identification of a structure subjected to seismic excitation. Yang et al. [15] also proposed an adaptive EKF approach which is capable of tracking the structural parameters, such as the stiffness and damping as well as unknown inputs. The adaptive technique enables the algorithm to identify the variations of structural parameters due to damage. The accuracy of EKF depends on the simplicity of the linear system contaminated by Gaussian noise. However, when either the under-study dynamical system is highly nonlinear or the noise is considerably non-Gaussian, the EKF may not be able to perform well. Therefore, in order to address the above challenges, a combination of the non-parametric modelling techniques and the ensemble Kalman filter (EnKF) has been introduced by Ghanem et.al [16]. EnKF uses the same corrector equation as the original Kalman filter, except that the gain is calculated from the error covariance provided by the ensemble of model states. The algorithm was able to detect both damage location and time of occurrence despite of measurement and modelling noise. Also, a comparison between ensemble and extended Kalman filters was presented.

Another approach to tackle the aforementioned problem is the Unscented Kalman Filter (UKF). UKF first is introduced by Julier et.al [17] and it utilises a deterministic “sampling” technique to measure the mean and covariance terms. First 2L+1 sigma points (L is the state dimension), need to be chosen based on a square-root decomposition of the prior covariance. Then a weighted mean and covariance is recovered by propagation of these sigma points through the true non-linear functions without approximation. Figure 1 shows a simple illustration of the technique for a 2-dimensional system which will be explained in details later.

Ungarala [18] developed the iterated forms of EKF and UKF (IEKF, IUKF), which can be thought as an estimator of the conditional mode that employs an approximate Newton–Raphson iterative scheme to determine the maximum value of the probability density function (pdf).

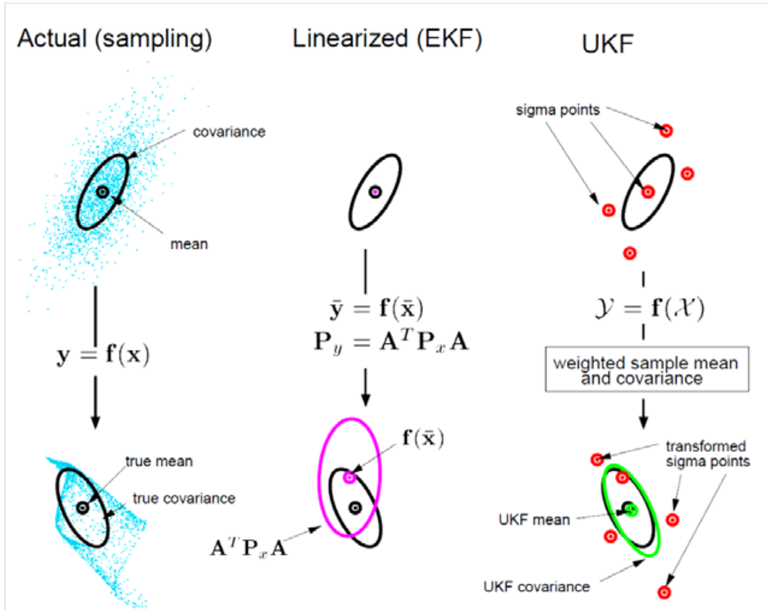

Fig. 1. Example of mean and covariance propagation [17].

In this study, the capability of four aforementioned algorithms, i.e. EKF, IEKF, UKF and IUKF in identifying the structural parameters, are compared by considering some numerical examples, including one nonlinear structural system with complex Jacobian matrix. The robustness and sensitivity of the methods to the measurement noise level and initial guesses of state vector will also be examined. To the authors' best knowledge, such an investigation has hitherto not been reported in the open literature.

2. Principles of EKF, IEKF, UKF and IUKF

To explain the principles of the aforementioned algorithms, we first consider a general dynamical system whose nonlinear state space equation with added noise is described by

$$\dot{x} = f\big(x(t)\big) + \mathrm{v}(\mathrm{t}) \tag{1}$$

where $\mathrm{v}(\mathrm{t})$ represents the process noise with covariance matrix Q(t). The nonlinear observation equation at time $t = k\Delta t$ can also be expressed as:

$$y_k = h(x_k) + \eta_k \tag{2}$$

where η_k shows the measurement noise with R_k. Equation (1) can be rewritten in a discrete form as follows

$$\begin{gathered} x_{k+1} = F(x_{k0}) + \mathrm{v_k} \\ y_k = h(x_k) + \eta_k \end{gathered} \tag{3}$$

where $\mathrm{v_k}$ is the process noise vector with corresponding covariance matrix Q_k. By integrating Eq. (1), one obtains the function F

$$F(x_k) = x_k + \int_{k\Delta t}^{(k+1)\Delta t} f(x(t))dt. \tag{4}$$

To obtain a recursive estimation of x_k, one of the algorithms described below may be used.

2.1. Extended Kalman Filter (EKF)

In the extended Kalman filter method, an initial estimate of the system's state is first predicted and then modified using observed and collected measurements ('measurement update' step). The state prediction $\hat{x}_k^-$ and corresponding covariance can be calculated as:

$$\hat{x}_k^{\,-} = \hat{x}_{k-1} + \int_{(k-1)\Delta t}^{(k)\Delta t} f(x(t))dt \tag{5}$$

$$P_k^- = \emptyset_k P_{k-1} \emptyset_k^{\,T} + Q_{k-1} \tag{6}$$

In Eq. (6), $\emptyset_{\mathrm{k}}$ is the state transition matrix and is found from:

$$\emptyset_k = I + \Delta t \left[\frac{\partial f(x(t))}{\partial x(t)}\right]_{x(t)=\hat{x}_{k-1}} \tag{7}$$

The predicted measurement is estimated as

$$\hat{Y}_k = h(\hat{x}_k^{\,-}) \tag{8}$$

Thus, in the measurement update step,

$$\begin{gathered} \hat{x}_k = \hat{x}_k^{\,-} + K_k(Y_k - \hat{Y}_k) \\ P_k = [I - K_k H_k]P_k^-[I - K_k H_k]^T + K_k R_k K_k^{\,T} \\ K_k = P_k^- H_k^{\,T}[H_k P_k^- H_k^T + R_k]^{-1} \end{gathered} \tag{9}$$

where K_k is the Kalman gain matrix at time step k and H_k is the linearised coefficient matrix of the observation equation given as:

$$H_k = \left[\frac{\partial \mathrm{h(x)}}{\partial x}\right]_{x=\hat{x}_k^{\,-}} \tag{10}$$

2.2. Iterated Extended Kalman Filter (IEKF)

In order to make the EKF more robust to the noise level and initial estimate of the state vector, the following iteration process is considered to be added to the standard EKF algorithm after the state prediction $\hat{x}_k^-$ and the corresponding covariance are estimated:

$$\begin{gathered} \hat{x}_{k,0} = \hat{x}_k^-, \quad P_{k,0} = P_k^- \\ \hat{x}_{k,j+1} = \hat{x}_k^- + K_{k,j}[y_k - h(\hat{x}_{k,j}) - H_{k,j}(\hat{x}_k^- - \hat{x}_{k,j})] \\ P_{k,j} = (I - K_{k,j}H_{k,j})P_k^-, \end{gathered} \tag{11}$$

where

$$\begin{gathered} H_{k,j} = \frac{\partial h(x)}{\partial x}|_{x=\hat{x}_{k,j}} \\ K_{k,j} = P_k^- H_{k,j}^T (H_{k,j} P_k^- H_{k,j}^T + R_k)^{-1}. \end{gathered} \tag{12}$$

This process will be terminated if the inequality $\|\hat{\mathrm{x}}_{\mathrm{k,j+1}} - \hat{\mathrm{x}}_{\mathrm{k,j}}\| \leq \mathrm{V_{th}}$ is satisfied, where $\mathrm{V_{th}}$ is the predetermined threshold. After N iterations (N should be chosen by user), the ultimate estimated state and corresponding covariance matrix are:

$$\hat{x}_k = \hat{x}_{k,N}, \qquad P_k = P_{k,N} \tag{13}$$

2.3. Unscented Kalman Filter (UKF)

The level of computational complexity of UKF is the same as EKF. However, it does not require the calculation of Jacobians or Hessians, and its accuracy is of second-order, whereas EKF can only reach a first order accuracy. The UKF estimation algorithm is explained in the following steps:

Step 1: Sigma Point Calculation

At time k-1, a set of deterministic sample points with related weights are calculated as;

$$\chi_{0,k-1} = \overline{x}_{k-1}$$
$$\chi_{i,k-1} = \overline{x}_{k-1} + (\sqrt{(L+\gamma)P_{k-1}})_i, \qquad i = 1,2,..,L \tag{14}$$
$$\chi_{i,k-1} = \overline{x}_{k-1} - (\sqrt{(L+\gamma)P_{k-1}})_{i-L}, \qquad i = L+1, L+2, \ldots, 2L$$

$$w_0^{(m)} = {}^{\gamma}\!/_{(L+\gamma)}$$
$$w_0^{(c)} = {}^{\gamma}\!/_{(L+\gamma)} + (1 - \alpha^2 + \beta) \tag{15}$$
$$w_i^{(m)} = w_i^{(c)} = {}^{1}\!/_{\{2(L+\gamma)\}}, \quad i = 1,2,\ldots,2L$$

where L is the dimension of x; χ_i and w_i denote sigma point and corresponding weight, respectively; $\gamma = \alpha^2(L+\kappa) - L$ is a scaling parameter; α identifies the spread of the sigma points around $\bar{x}$, and usually it is a small positive value (0.0001≤ α ≤ 1), κ is a secondary scaling parameter which is usually set to 0; β is used to incorporate the prior distribution of x (for a Gaussian distribution β =2 is optimal); $(\sqrt{P})_i$ denotes the i^{th} row of the matrix square root.

Step 2: Time Update

After the sample points are transmitted through the nonlinear equations, the mean and covariance are predicted as follows:

$$\chi_{k|k-1} = f(\chi_{k-1})$$
$$\hat{x}_k^- = \sum_{i=0}^{2L} w_i^{(c)} \chi_{i,k|k-1}$$
$$P_k^- = \sum_{i=0}^{2L} w_i^{(c)} \left[\chi_{i,k|k-1} - \hat{x}_k^-\right]\left[\chi_{i,k|k-1} - \hat{x}_k^-\right]^T + Q_k$$
$$\chi_{k|k-1}^* = \left[\chi_{0:2L,k|k-1}, \qquad \chi_{0,k|k-1} + \nu\sqrt{Q_k}, \qquad \chi_{0,k|k-1} - \nu\sqrt{Q_k}\right] \tag{16}$$
$$Y_{k|k-1}^* = h\left(\chi_{k|k-1}^*\right)$$
$$\hat{y}_k^- = \sum_{i=0}^{2L^\alpha} w_i^{*(m)} Y_{i,k|k-1}^*$$
$$P_{yy,k} = \sum_{i=0}^{2L^\alpha} w_i^{*(c)} \left[Y_{i,k|k-1}^* - \hat{y}_k^-\right]\left[Y_{i,k|k-1}^* - \hat{y}_k^-\right]^T + R_k$$
$$P_{xy,k} = \textstyle\sum_{i=0}^{2L^\alpha} w_i^{*(c)} \left[\chi_{i,k|k-1}^* - \hat{x}_k^-\right]\left[Y_{i,k|k-1}^* - \hat{y}_k^-\right]^T,$$

where L^α =2L, $\nu = \sqrt{L+\gamma}$; $w_i^{*(c)}$i and $w_i^{*(m)}$are computed in the same way as Eq. (15) by replacing L with L^α. It should be mentioned that in Eq. (16), additional points derived from the matrix square root of the process noise covariance Q are added to the sigma points. The idea behind this is to consider the effect of the process noise to the observed sigma points Y. More details can be found in the paper by Van Der Merwe [19].

Step 3: Measurement Update

The Kalman gain is computed to update the state and covariance as follow,

$$K_k = P_{xy,k} P_{yy,k}^{-1}$$

$$\hat{x}_k = \hat{x}_k^- + K_k (y_k - \hat{y}_k^-) \tag{17}$$

$$P_k = P_k^- - K_k P_{yy,k} K_k^T$$

The abovementioned three steps summarise the procedure of UKF algorithm. By using an initial condition $\bar{x}_0 = E[x_0]$ and $P_0 = E[(x_0 - \bar{x}_0)(x_0 - \bar{x}_0)^T]$, the filtering approach can be recursively implemented.

2.4. Iterated Unscented Kalman Filter (IUKF)

In view of the development of IEKF and the desire to improve the accuracy of UKF, a natural idea is to implement the iterations in UKF. However, special steps should be taken to make the iterated filter perform as good as possible. In following steps, the IUKF is explained in detail.

Step 1: for each instant, when $k \geq 1$, evaluate the state estimate $\hat{x}_k$, and corresponding covariance matrix P_k through Eq. (2.14 to 2.17),

Step 2: Let $\hat{x}_{k,0} = \hat{x}_k^-$, $P_{k,0} = P_k^-$ and $\hat{x}_{k,1} = \hat{x}_k$, $P_{k,1} = P_k$. Also let $g = 1$ and $j = 2$.

Step 3: Sigma points generation:

$$\chi_{i,j} = \left[\hat{x}_{k,j-1}\,, \qquad \hat{x}_{k,j-1} + \sqrt{(L+\gamma)P_{k,j-1}}, \qquad \hat{x}_{k,j-1} - \sqrt{(L+\gamma)P_{k,j-1}}\right]_i \tag{18}$$

Step 4: Recalculate Eqs. (16) and (17) as follows:

$$\hat{x}_{k,j}^- = \sum_{i=0}^{2L} w_i^{(m)} \chi_{i,j}$$

$$Y_{i,j} = h(\chi_{i,j})$$

$$\hat{y}_{k,j}^- = \sum_{i=0}^{2L} w_i^{(m)} Y_{i,j}$$

$$P_{yy,k,j} = \sum_{i=0}^{2L} w_i^{(c)} \left[Y_{i,j} - \hat{y}_{k,j}^-\right]\left[Y_{i,j} - \hat{y}_{k,j}^-\right]^T + R_k \tag{19}$$

$$P_{xy,k,j} = \sum_{i=0}^{2L} w_i^{(c)} \left[\chi_{i,j} - \hat{x}_{k,j}^-\right]\left[Y_{i,j} - \hat{y}_{k,j}^-\right]^T$$

$$K_{k,j} = P_{xy,k,j} P_{yy,k,j}^{-1}$$

$$\hat{x}_{k,j} = \hat{x}_{k,j}^- + g.K_{k,j}(y_k - \hat{y}_{k,j}^-)$$

$$P_{k,j} = P_{k,j-1}^- - K_{k,j} P_{yy,k,j} K_{k,j}^T$$

where index j indicates the j^{th} iteration; $Y_{i,j}$ denotes the i^{th} component of Y_j.

Step 5: Define the following three equations: (i) $\hat{y}_{k,j} = h(\hat{x}_{k,j})$, (ii) $\tilde{x}_{k,j} = \hat{x}_{k,j} - \hat{x}_{k,j-1}$, and (iii) $\tilde{y}_{k,j} = y_k - \hat{y}_{k,j}$

Step 6: if the following inequality holds:

$$\tilde{x}_{k,j}^T P_{k,j-1}^{-1} \tilde{x}_{k,j} + \tilde{y}_{k,j}^T R_k^{-1} \tilde{y}_{k,j} < \tilde{y}_{k,j-1}^T R_k^{-1} \tilde{y}_{k,j-1}, \tag{20}$$

and if $j \leq N$, then set $g = \eta.g$, $j = j + 1$ and return to Step 3; otherwise proceed to Step 7.

Step 7: stop if the inequality (20) is not satisfied or if j is too large (j>N) and set $\hat{x}_k = \hat{x}_{k,j}$, $P_k = P_{k,j}$.

For positive definite matrices $P_{k,j}$, $P_{k,j-1}$ and $P_{yy,k,j}$ assume that $\lim_{j\to\infty} K_{k,j} \neq 0$, then according to Eq. (19), we have $P_{k,j} < P_{k,j-1}$ for any $j = 1,2,.. < \infty$. Based on the fact that each element of the matrix $P_{k,j}$ is bounded, it is easy to know that $\lim_{j\to\infty} P_{k,j} = \lim_{j\to\infty} P_{k,j-1}$. With this premise, it can be inferred from Eq. (19) that $\lim_{j\to\infty} K_{k,j} = 0$, which violates the assumption that $\lim_{j\to\infty} K_{k,j} \neq 0$. However, the assumption is not true and the only possibility is that $\lim_{j\to\infty} K_{k,j} = 0$. Now suppose that $K_{k,j} \to 0$ when $j > N$, then from Eq. (19), we have $\hat{x}_{k,j} \to \hat{x}_{k,j}^{-} = \hat{x}_{k,j-1}$ and $P_{k,j} \to P_{k,j-1}$, which shows the convergence of the under-study algorithm as the iteration process proceeds.

From Eq. (19), we can find out the state estimate after N iterations is $\hat{\mathrm{x}}_{\mathrm{k,N}} = \hat{\mathrm{x}}_{\mathrm{k,N}}^{-} + \eta^{\mathrm{N-1}}\mathrm{K}_{\mathrm{k,n}}(\mathrm{y}_{\mathrm{k}} - \hat{\mathrm{y}}_{\mathrm{k,N}}^{-})$. Since for a large N, $\eta^{\mathrm{N-1}} \to 0$, therefore $\hat{\mathrm{x}}_{\mathrm{k,N}} \to \hat{\mathrm{x}}_{\mathrm{k,N}}^{-} = \hat{\mathrm{x}}_{\mathrm{k,N-1}}$ if N is large enough and the decaying factor η is between 0 and 1. One can also conclude that iteration process will converge to a solution; although, the convergence speed is influenced by the factor η.

Compared with UKF, the IUKF, through corrections of the measurement, can adjust the state estimate to converge to the true value through corrections of the measurement. Therefore, a smaller state error can be expected, after the iteration stops. Moreover, the response of the proposed filter to new measurements is as quick as possible with the adjustment of state and covariance matrix. This feature can help in making a faster convergence speed where the initial error is large [20,21].

3. Numerical Simulations

3.1. SDOF nonlinear hysteretic structure

As first case study, a single degree of freedom (SDOF) nonlinear hysteretic Bouc-Wen structure, is considered here and is subjected to earthquake acceleration $\ddot{x}_g$ (Figure 2). The governing equation of motion is given by

$$m\ddot{x}(t) + c\dot{x} + kr(t) = -m\ddot{x}_g(t) \tag{21}$$

where $r(\dot{x}, x)$ represents the Bouc-Wen model and it is expressed by

$$\dot{r} = \dot{x} - \beta|\dot{x}||r|^{\alpha-1}r - \gamma\dot{x}|r|^{\alpha} \tag{22}$$

In Eq. (22), c is the damping coefficient, k is the stiffness, and β, γ and α are the hysteretic parameters. The parametric values used here for the simulation purpose are as follows: m=1 kg, c=0.3 Ns/m, k=9 N/m, β=2, $\gamma = 1$ and $\alpha = 2$. Also the ground excitation, $\ddot{x}_g$, which is considered here is the El-Centro earthquake of 1940 with a peak ground acceleration of 0.15 g (PGA=0.15g). The acceleration of the mass, $\ddot{x}$, and ground, $\ddot{x}_g$, is measured using the installed sensors and the unknown parameters are taken as c, k, β, α and γ. Moreover, in order to check the robustness of the algorithm to noise, a white noise process with different root mean square (RMS) noise-to-signal ratios is added to both the structural acceleration response and the earthquake ground acceleration. The system responses of the displacement, velocity, and acceleration were obtained by solving differential Eq. (21) using the fourth-order Runge–Kutta integration method.

The objective is to estimate the unknown parameters as well as the displacement, velocity and r(t) signals. Therefore, the state vector to be estimated is defined as:

$$X = [x_1,\ x_2,\ x_3,\ x_4,\ x_5,\ x_6,\ x_7,\ x_8\ ]^T = [x, \dot{x}, r, c, k, \beta, \gamma, \alpha].$$

Equations (21) and (22) may be rewritten in the form of state space as follows:

$$f(X(t),u(t)) = \begin{bmatrix} x_2 \\ -\ddot{x}_g - \dfrac{x_2x_4 + x_3x_5}{m} \\ x_2 - x_6|x_2||x_3|^{x_8-1}x_3 - x_7x_2|x_3|^{x_8} \\ 0 \\ 0 \\ 0 \\ 0 \\ 0 \end{bmatrix} \tag{23}$$

The system equation, shown above, clearly demonstrates a strong nonlinear behaviour. If both acceleration response and excitation are measurable, then the observation equation, which is the absolute acceleration of the mass m, can be expressed as:

$$y = \ddot{x} + \ddot{x}_g + v = -\frac{c\dot{x} + r}{m + v} = -\frac{x_2x_4 + x_3x_5}{m} + v \tag{24}$$

The simulation is carried out using 2% added root mean square (RMS) noise-to-signal ratio and initial guesses of $X_0 = [0, 0, 0, 0.2, 5, 0, 0.5, 1]$. The identification of the parameters during the earthquake is depicted in Fig. 3 while the estimated hysteretic loops between 4 to 8 seconds, using the four aforementioned algorithms are shown in Fig. 4.

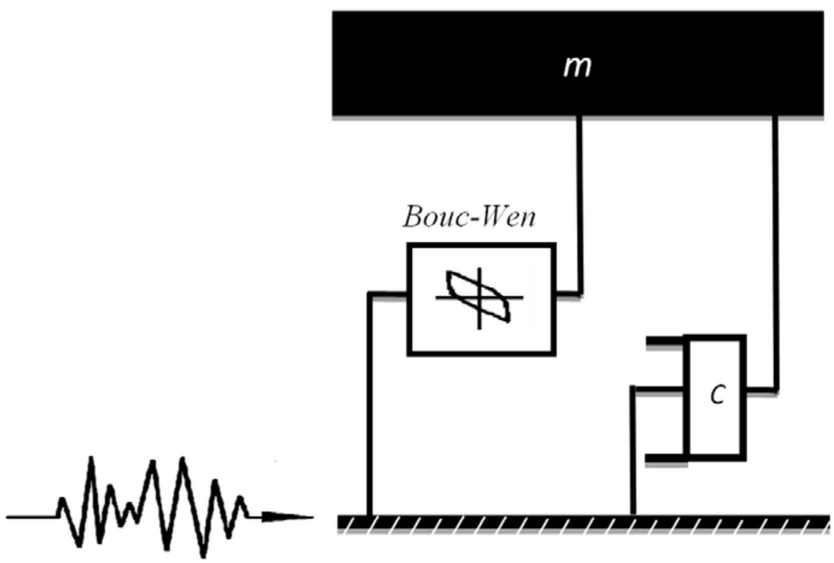

Fig. 2. SDOF nonlinear hysteretic system

As can be observed from Fig. 3, the IEKF and IUKF have better convergence speed and accuracy compared to their standard forms and IUKF shows the best performance among all methods in terms of both accuracy and convergence speed. It is worth noting that the former IEKF has not been applied to structural parameters identification before.

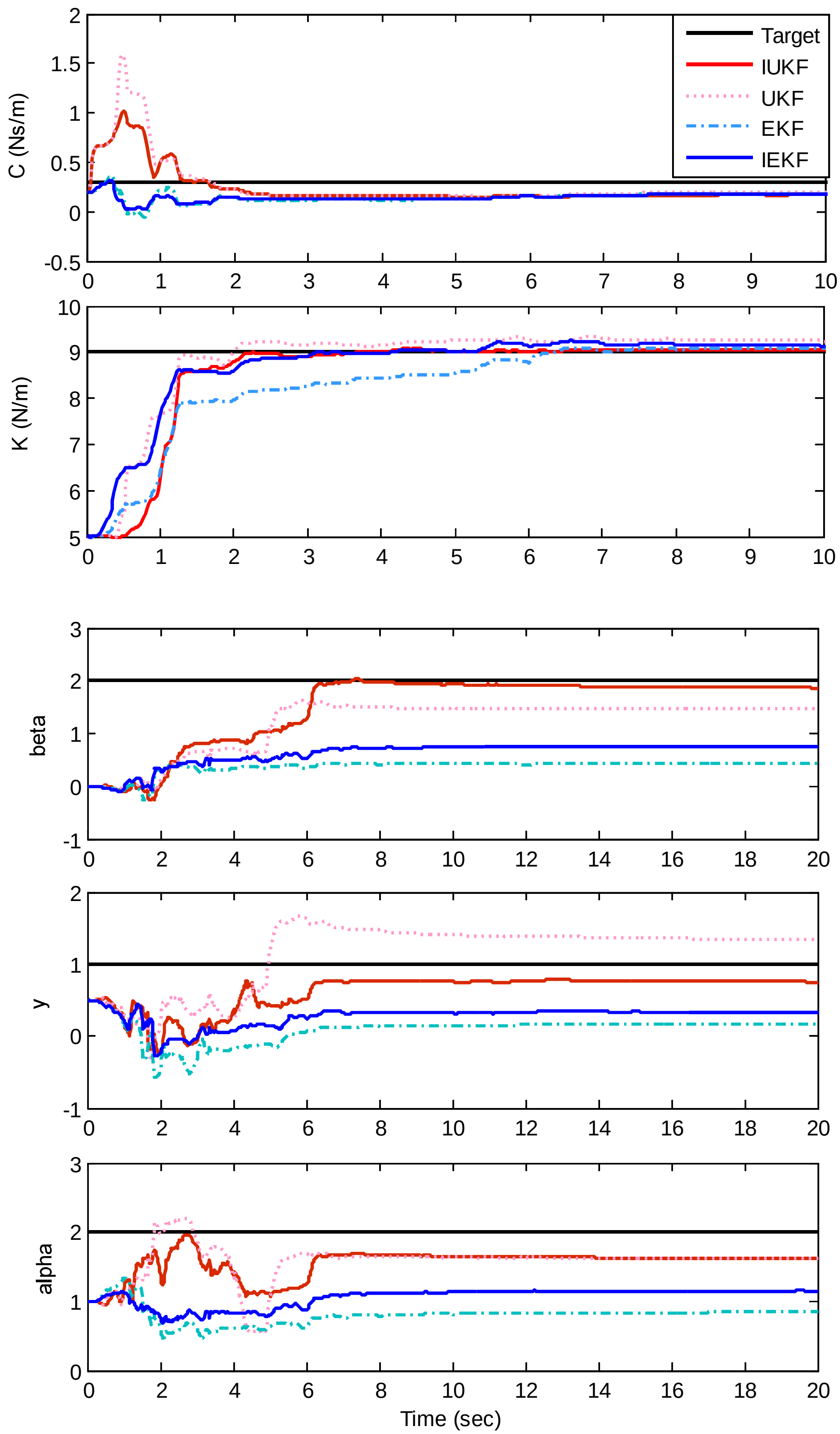

Fig. 3. Parameters estimation for SDOF nonlinear system, noise level 2% RMS.

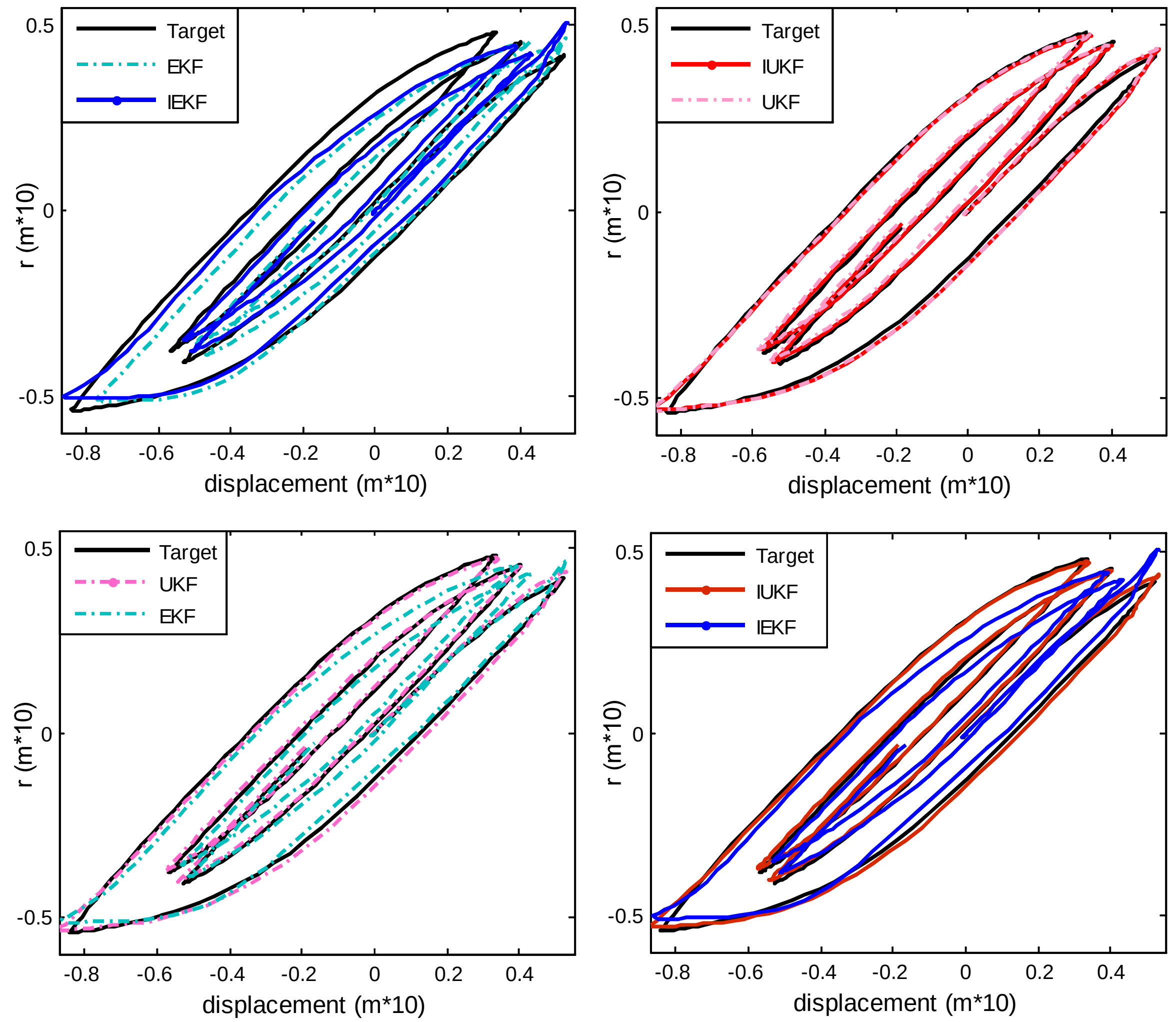

Fig. 4. Estimated hysteretic loops for the Bouc–Wen system, noise level 2% RMS

3.2. 2DOF linear structural system

Next, consider a two-degree of freedom (2DOF) structural system subjected to an earthquake excitation as shown in Fig. 5. The governing equations of motion are given by

$$\begin{gathered} m_1\ddot{x}_1 + c_1\dot{x}_1 + c_2(\dot{x}_1 - \dot{x}_2) + k_1x_1 + k_2(x_1 - x_2) = -m_1\ddot{x}_g \\ m_2\ddot{x}_2 + c_2(\dot{x}_2 - \dot{x}_1) + k_2(x_2 - x_1) = -m_2\ddot{x}_g, \end{gathered} \tag{25}$$

in which $m_1 = m_2 = 1\ kg$, $c_1 = 0.6\ Ns/m$, $c_2 = 0.5\ Ns/m$, $k_1 = 12\ N/m$, and $k_2 = 10\ N/m$. Although the system is linear; the estimation of the unknown parameters together with the states of the system is a nonlinear identification problem. The same earthquake signal as in the previous case study is used as the excitation to the structure. Here, the acceleration response of structure and the earthquake signal are considered to be known. The purpose here is to also predict the stiffness and damping of different storeys and estimate the velocity and displacement signals of different floors. Thus, the state vector to be tracked is defined as:

$$X = [X_1, X_2, X_3, X_4, X_5, X_6, X_7, X_8\,]^T = [x_1, \dot{x}_1, x_2, \dot{x}_2, k_1, k_2, c_1, c_2].$$

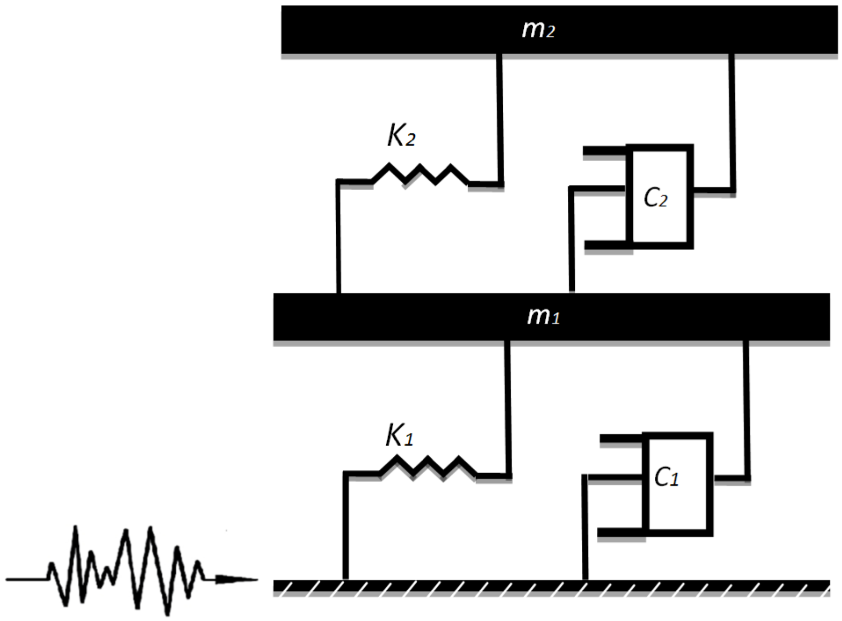

Fig. 5. 2DOF linear system

In the first run, a noise level of 1% RMS is added to both measured signals and ground acceleration. The initial state vector is also thought to be $X_0 = [0.0001, 0.0001, 0.0001, 0.0001, 5, 5, 0.3, 0.3]$. The identified parameters during the first 8 seconds of the earthquake are illustrated in Fig. 6. As it can be seen, UKF and IUKF have better performances than EKF and IEKF in the beginning of the process. However, all the methods converge to almost the same values after 4 seconds. It is interesting to note that although the performance of IEKF was expected to be always better than EKF, the results show that EKF can track the damping values with less fluctuations than IEKF. The reason is that when the local linearization condition is unconditionally met [22,23], i.e., the estimated state of the system is close enough to the actual value, then IEKF performs better than EKF. However, this assumption is not always true as in many applications, the initial estimate errors is large. Also, from the updated equations, it is clear that the state correction in each iteration related to the measurement error. However, since the measurement error cannot be zero as ideal cases, therefore, the convergence of iterations depends on the accuracy of measurements. Moreover, a proper choice of the threshold V_{th} is another important factor which affects the performance of iterated algorithm. In this study, a threshold of 0.08 has been used to simulate the IEKF.

To check the robustness and sensitivity of the algorithms to noise level and the initial state vector, a second simulation is performed using a noise level of 5% RMS and initial state vector of $X_0 = [0.0001, 0.0001, 0.0001, 0.0001, 2.8, 2.8, 0.15, 0.15]$. Results are shown in Fig. 7 in which, the performances of the four identification techniques are compared with one another.

As can be found from Fig. 7, although IEKF is an improved version of EKF, it still cannot perform well when the initial values of the unknown parameters are far from the real ones. IUKF, on the other hand, tracks the parameters with good accuracy, which is even better than UKF.

Table 1 shows the final identified parameters of the structure with different noise levels and initial state vector. The best result in each section is bold faced. From the results, the superiority of IUKF over the other methods is clearer when more noise level is superimposed to the signals and the initial state vector is far from the real values.

4. Conclusion

A comparison study have been carried out on application of four different Kalman Filtering methods, i.e EKF, IEKF, UKF and IUKF for estimating the states and parameters of linear and nonlinear civil structures in real-time. The governing equation in both numerical examples, was nonlinear and in one of the cases, the structure also exhibited highly hysterical structural nonlinearity. The numerical results showed that, the performance of EKF and UKF are improved by their corresponding iterated versions, i.e. IEKF and IUKF. However, when the initial state estimate of the system is not close to the target value and consequently the initial measurement error is large or if threshold value V_{th} is not chosen properly, IEKF shows a weaker performance as compared to the standard

EKF. The UKF method, on the other hand, has shown to be superior to EKF and IEKF in the structural identification applications. However, when the structure is highly nonlinear or the initial estimate of the unknown parameters are not close to actual values, and also if the measurement signals are contaminated with high noise level, IUKF is the best one among the four algorithms considered, in terms of robustness, convergence speed and tracking accuracy.

It is also worth noting that no paper has been found in the open literature on the application of IEKF to structural parameters identification. Also, such comparison between these four aforementioned algorithms in finding the structural parameters has not been studied before.

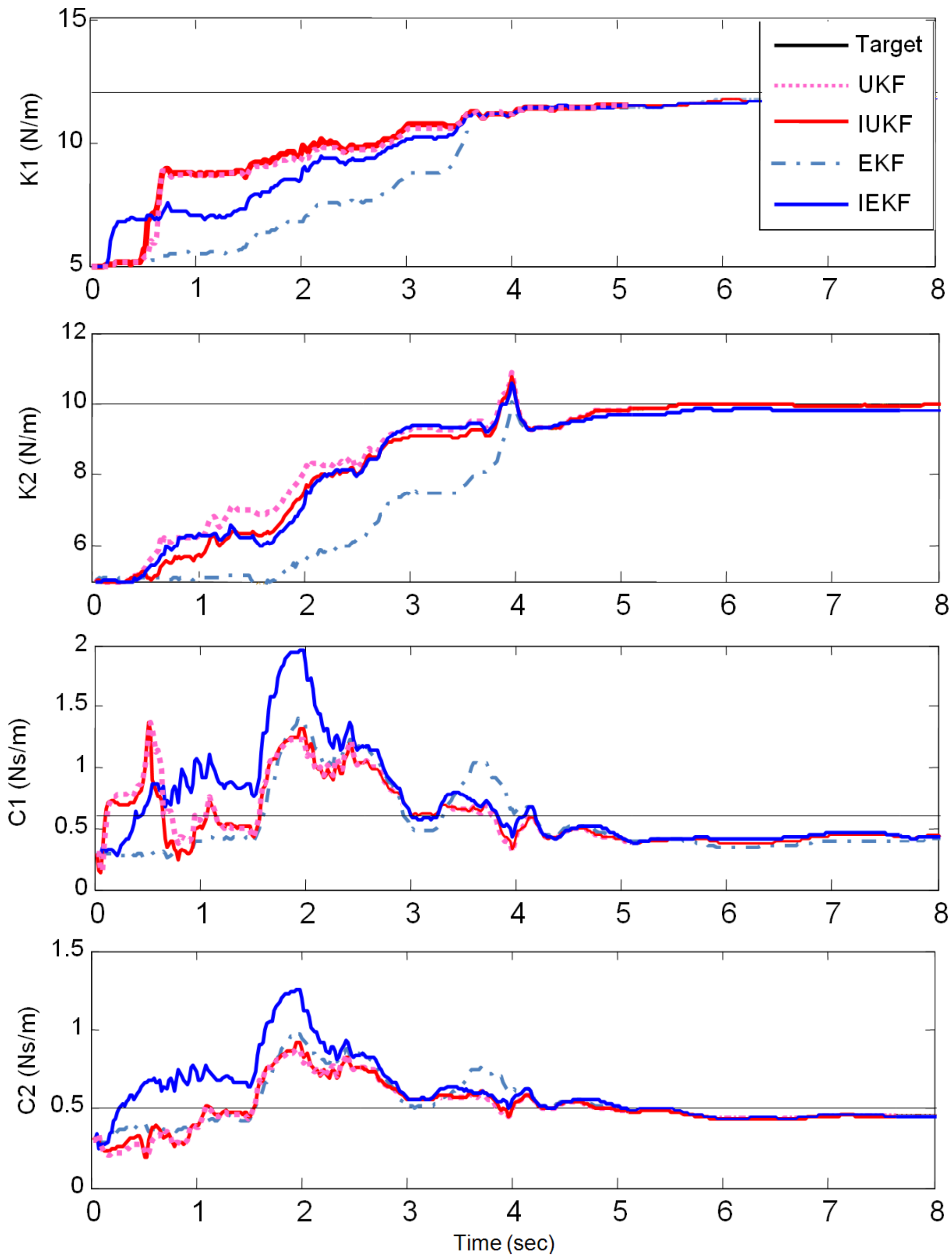

Fig. 6. Parameters estimation for 2-DOF linear system, noise level 1% RMS and $\mathbf{X_0} = [\mathbf{0.0001}, \mathbf{0.0001}, \mathbf{0.0001}, \mathbf{0.0001}, \mathbf{5}, \mathbf{5}, \mathbf{0.3}, \mathbf{0.3}]$.

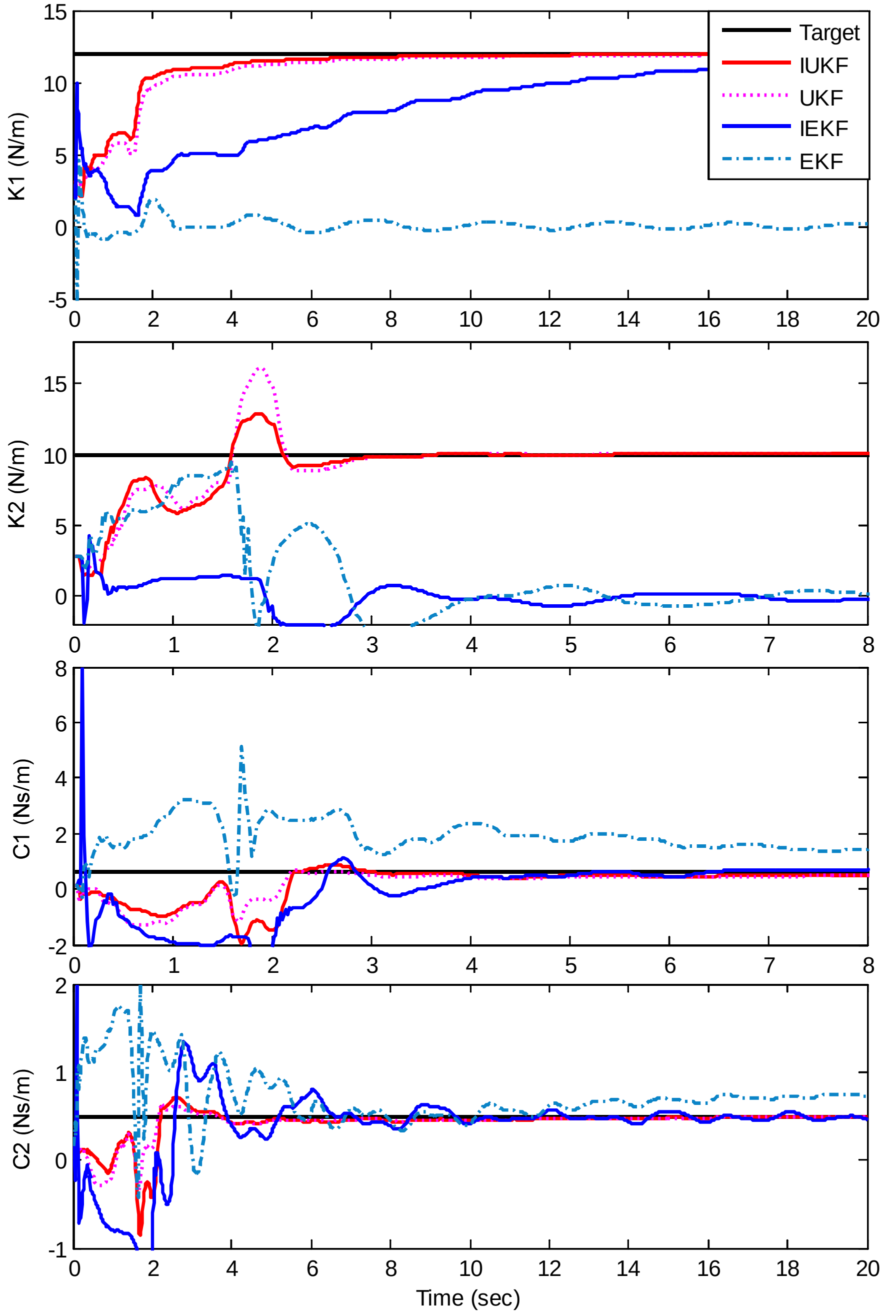

Fig. 7. Parameters estimation for 2-DOF linear system, noise level 5% RMS, and
$\mathbf{X_0} = [\mathbf{0.0001}, \mathbf{0.0001}, \mathbf{0.0001}, \mathbf{0.0001}, \mathbf{2.8}, \mathbf{2.8}, \mathbf{0.15}, \mathbf{0.15}]$.

Table 1. Estimation results for 2DOF linear system.

Starting Point	Noise Level	Identification Method		**K_1(N/m)**	**K_2(N/m)**	**C_1(N s/m)**	**C_2 (N s/m)**
			Exact:	12	10	0.6	0.5
$X_0 = [0,0,0,0.5,5,0.3,0.3]$	1%	EKF	Estimated:	11.9553	10.0033	0.5595	0.4912
			Error (%):	0.37	0.03	6.75	1.76
		IEKF	Estimated:	11.9688	9.9974	0.5855	0.4852
			Error (%):	0.26	0.026	**2.42**	2.96
		UKF	Estimated:	11.9916	10.0010	0.5808	0.4900
			Error (%):	0.07	**0.01**	3.2	2
		IUKF	Estimated:	11.9917	10.0024	0.5812	0.4914
			Error (%):	**0.069**	0.024	3.13	**1.74**
$X_0 = [0,0,0,2.8,2.8,0.15,0.15]$	5%	EKF	Estimated 1:	0.159	-0.1226	1.18	0.73
			Error (%):	98.66	101	96.67	46.00
		IEKF	Estimated:	11.518	0.123	0.76	0.458
			Error (%):	4.017	98.77	26.67	8.4
		UKF	Estimated:	11.957	10.049	0.581	0.490
			Error (%):	0.358	0.49	3.16	**2**
		IUKF	Estimated:	11.977	10.047	0.592	0.485
			Error (%):	**0.192**	**0.47**	**1.33**	3

References

1. C. R. Farrar, K. Worden, An introduction to structural health monitoring. *Philosophical Transactions of the Royal Society A: Mathematical, Physical and Engineering Sciences* 365 (2007) 303-315.
2. C. H. Loh, C. Y. Lin, Application of offline and online identification techniques to building seismic response data, *Earthquake engineering & structural dynamics* 25 (3) (1996) 269-290.
3. C. H. Loh, C. Y. Lin and C. C. Huang, Time domain identification of frames under earthquake loadings. *Journal of Engineering Mechanics*, 126 (2000) 693-703.
4. S. Zheng, L. Zheng-Qian and W. Hong-Ta, A genetic fuzzy radial basis function neural network for structural health monitoring of composite laminated beams. *Expert Systems with Applications* 38.9 (2011) 11837-11842.
5. B. Samali, J. Li, F. C. Choi and K Crews, Application of the damage index method for plate-like structures to timber bridges, *Structural Control and Health Monitoring* 17(8) (2010) 849-871.
6. T. Sato, K. Qi, Adaptive Kalman filter: its application to structural identification. *Journal of Engineering Mechanics* **124** (1998) 1233-1240.

7. S. Li, Y. Suzuki, M. Noori, Improvement of parameter estimation for non-linear hysteretic systems with slip by a fast Bayesian bootstrap filter. *International Journal of Non-Linear Mechanics* **39** (2004) 1435-1445.

8. S. Masri, A. Smyth, A. Chassiakos, T. Caughey and N. Hunter, Application of neural networks for detection of changes in nonlinear systems. *Journal of Engineering Mechanics* **126** (2000), 666-676.

9. C. Zang, M. Friswell and Imregun, Structural damage detection using independent component analysis, *Structural Health Monitoring* **3** (2004) 69-83.

10. J. Zapico, K. Worden and F. Molina, Vibration-based damage assessment in steel frames using neural networks, *Smart materials and structures* **10** (2001) 553.

11. M. Vafaei, B. A. Azla and B. A. R. Ahmad, Real-time seismic damage detection of concrete shear walls using artificial neural networks, *Journal of Earthquake Engineering* **17**(1) (2013) 137-154.

12. H. Kim, H. Melhem, Damage detection of structures by wavelet analysis, *Engineering Structures* 26 (2004) 347-362.

13. M. Wu, A.W. Smyth, Application of the unscented Kalman filter for real-time nonlinear structural system identification, *Structural Control and Health Monitoring* **14** (2007) 971-990.

14. M. Hsohiya, E. Saito, Structural identification by extended Kalman filter, *Journal of Engineering Mechanics* **110** (1984) 1757-1770.

15. J. Yang, S. Pan and H. Huang, An adaptive extended Kalman filter for structural damage identifications II: unknown inputs, *Structural Control and Health Monitoring* **14** (2007) 497-521.

16. R. Ghanem, G. Ferro, Health monitoring for strongly nonlinear systems using the Ensemble Kalman filter, *Structural Control and Health Monitoring* **13** (2006) 245-259.

17. S. J. Julier, J. K. Uhlmann, New extension of the Kalman filter to nonlinear systems, *AeroSense97 International Society for Optics and Photonics* (1997).

18. S. Ungarala, On the iterated forms of Kalman filters using statistical linearization, *Journal of Process Control* **22** (2012) 935-943.

19. R. Van Der Merwe, Sigma-point Kalman filters for probabilistic inference in dynamic state-space models. *University of Stellenbosch* (2004).

20. E. N. Chatzi, A. W. Smyth, The unscented Kalman filter and particle filter methods for nonlinear structural system identification with non-collocated heterogeneous sensing, *Structural Control and Health Monitoring* **16** (2009) 99-123.

21. Z. Xie, J. Feng, Real-time nonlinear structural system identification via iterated unscented Kalman filter, *Mechanical Systems and Signal Processing* **28** (2012) 309-322.

22. G. Fucheng, S. Zhongkang and H. Kan, A modified covariance extended Kalman filtering algorithm in passive location, *IEEE International Conference on Robotics, Intelligent Systems and Signal Processing* (2003).

23. G. Xiangyi, The Study of challenge technology of single observer passive location and tracking using frequency rate and differential direction of arrival. *Changsha: National University of Defence Technology* (2004) 10-28.